Superparamagnetic Iron Oxide Nanoparticles Induce Apoptosis in HT-29 Cells by Increasing ROS and Damaging DNA

Ali Ghorbani Ranjbary
Tehran University: University of Tehran
Golnaz Karbalaei Saleh
Karaj Islamic Azad University
Mohammadreza Azimi (rezazimi87@gmail.com)
Islamic Azad University Saveh Branch https://orcid.org/0000-0003-0031-0028

Research Article

Keywords: Colon cancer, Fe3O4 nanoparticles, Apoptosis, Reactive oxygen species

Posted Date: June 16th, 2021

DOI: https://doi.org/10.21203/rs.3.rs-535697/v1

Abstract

Today, research into nanoparticles for diagnostic and therapeutic use in cancer is on the rise. In the present study, the effect of superparamagnetic iron oxide nanoparticles on the formation of apoptosis in HT-29 cells is investigated.

In this study, we investigated the mechanisms of apoptosis induced by superparamagnetic iron oxide nanoparticles after MTT assay and determining the appropriate dose of 2.5 µg / mL to induce apoptosis in HT-29 cells.

Superparamagnetic iron oxide nanoparticles increased the levels of ROS, Ca2 +, and DNA damage in HT-29 cells. Also, at the level of protein and mRNA, they increased the expression of Caspes 3 and 9 and significantly decreased Bcl-2 compared to the control group (P <0.0001).

Fe3O4 causes apoptosis in cancer cells by increasing the level of ROS and intracellular calcium, followed by increasing the expression of caspases 3 and 9 and decreasing the expression of Bcl-2, as well as direct DNA damage.

Introduction

Cancer has always been one of the most fundamental problems of human societies. Despite the vast amount of research and developments over the past decade, cancer remains one of the leading causes of death worldwide. According to recent statistics, cancer is the second leading cause of death in the world after cardiovascular disease [1–3]. Current treatments for cancer include chemotherapy, radiation, and surgery. However, these methods are not specific to cancer. Many researchers have found that a combination of two or three treatments often has better and more effective treatment results than a single treatment. However, in most cases, healthy cells also die and there can be side effects in the patient. Therefore, it is essential to explore new treatments for cancer control [4 and 5].

In recent years, nanotechnology has emerged as one of the major goals in the treatment of cancers. Its benefits in drug design include increased sensitivity to radiotherapy, protection from the adverse effects of radiotherapy, and increased tumor cell killing. Meanwhile, metal oxide nanoparticles have received a lot of attention for the treatment of cancer. Natural oxides of metals are present in large quantities in nature and their production is not very expensive. Hence, it directs research in this field toward the production of cost-effective pharmaceutical products and processing and synthesis of these nanoparticles can be one of the least expensive synthesis instructions [6–7]. Therefore, magnetic iron oxide nanoparticles are one of the most important metal nanoparticles that are used in a wide range of biomedical technologies and applications due to their biocompatibility, physicality, low toxicity, stability, cell cycle arrest, and magnetic properties [8, 9]. In addition, magnetic iron oxide nanoparticles have been shown to have cytotoxic properties in cancer cells [10, 11]. Magnetic iron oxide nanoparticles have been used in chemotherapeutic compounds in the treatment of various cancers such as blood, lung cancer, pancreatic cancer, and prostate cancer cells [12].

Previous studies have shown that magnetic nanoparticles can cause apoptosis in cells due to the production of oxygen free radicals and oxidative stress [15 – 13]. Despite extensive studies on the toxicity of nanomaterials on mitochondrial damage, oxidative stress, genome damage, alteration of cell cycle settings, and denaturation of proteins, the mechanism by which they act on body parts remains unknown. One of the possible mechanisms associated with nanoparticles is the formation of reactive oxygen species (ROS) and subsequently oxidative stress, which lead to changes in the amount of cellular calcium, occurrence of inflammatory cell responses, activation of transcription factors (p53 is a transcription factor), and increase in the production of cytokines, which eventually cause apoptosis [16–17]. Nanomaterials also play a key role in DNA damage, membrane destruction, and eventual cell death by causing oxidative stress and lipid peroxidation [18]. As such, they can lead to effective therapies resulting in the destruction of the tumor by minimizing treatment side effects [19]. Therefore, the purpose of this study was to investigate the mechanism of apoptosis formation in HT-29 cells by superparamagnetic iron oxide nanoparticles.

Materials And Methods

Synthesis of paramagnetic iron oxide nanoparticles: Superparamagnetic iron oxide nanoparticles were synthesized using the co-precipitation method (20, 21). Figure 1A shows the TEM and SEM images of paramagnetic iron oxide nanoparticles synthesized by co-precipitation.

MTT assay: MTT colorimetric method is one of the tests that is performed based on reduction and breaking of yellow tetrazolium crystals by the succinate dehydrogenase enzyme and formation of insoluble blue crystals. Biological evaluation of normal and cancer cells was examined. After cell culture, cell suspension (10^4 cells per ml) was implanted in 96-well microplates and treated for 24 hours in a CO_2 incubator at 37°C. Then, different concentrations of paramagnetic iron oxide nanoparticles were added to the wells containing the cells. A culture medium containing 1% DMSO (dimethyl sulfoxide) without nano-treatment was used as a negative control. Wells containing cells and nanoparticles were incubated for 24 hours. Then 20 µl of solution (MTT Sigma Aldridge, Germany) (5 mg / ml) was added to each well and incubated for another 3 hours. 100 µl of DMSO solution was added to each well and the culture plate was shaken for 10 minutes to dissolve the MTT violet precipitate. Then, by ELISA reading, the light absorption of the samples was measured at 570 nm [22].

Cell culture: In this study, HT-29 colon cancer cell line was used, which was prepared from Ferdowsi University of Mashhad Cell Bank, Iran. $RPMI_{1640}$ culture medium supplemented with 10% FBS serum was used for cell culture and treated at 37°C, 5% carbon dioxide, and 95% incubator moisture. The percentage of living cells was determined by cell staining using trypan blue. When the number of cells in the flask reached a density of about 80%, they were passaged. Finally, in the untreated control group and the treated group, 2.5 µg/mL of paramagnetic iron oxide nanoparticles was cultured for 48 hours.

Real-time and analysis: First, specific primers for 4 apoptosis-related genes (Bcl-2, Bax, Caspase 3, and Caspase9) were designed using the Beacon Designer v8 software (Table 1). Then, RNA was extracted

from the two studied groups using an RNA extraction kit (Dena Zist Asia (S-1010-1)), and after converting to cDNA, all biological samples (5 replications in the two studied groups) were placed in a Rotor-Gene Q 2.3.5 RT-PCR and 95°C cDNA denaturation temperature was performed for 10 minutes, then a 40-cycle period including 95°C in 10 seconds, 60°C in 20 seconds, 72°C in 20 seconds was used for (Bax, Bcl-2, Ccaspase3, and Caspase9) and reading. In this experiment, Yekta Tajhiz Azma (YTZ (Cost No: YT2551, Iran)) Master Mix and SYBR Green kits were used. At first, crew standard was performed for normalization of cDNA. Then, the melting curve and CT were analyzed in each sample.

Table 1
List of different RT-qPCR primers used in the study

Gene (ENST)	Sequence (5' – 3')	T_m (°C)	Length (bp)
Caspase 3 (ENST00000393585.6)	F: ATGGGAGCAAGTCAGTGGAC R: CGTACCAGAGCGAGATGACA	60	84
Caspase 9 (ENST00000469637.1)	F: GGCGGAGCTCATGATGTCTGTG R: TTCCGGTGTGCCATCTCCATCA	61	156
BCL-2 (ENSG00000126453)	F: GAGCGTCAACAGGGAGA R: GCCAGGAGAAATCAAACA	60	164
Bax (ENSG00000087088)	F: ACTAAAGTGCCCGAGCTGA R: ACTCCAGCCACAAAGATGGT	60	161
B-ACTIN (ENST00000515712.1)	F: CTACCTTCAACTCCATCA R: GAGCAATGATCTTGATCTTC	60	165

The initial analysis was performed using the GeneX v6.7 software and the results were all calculated based on Delta Delta CT and Log Two. Then they were statistically analyzed with the Graphpad Prism software version 8.

Western Blatting

To determine protein expression, Western blot analysis was performed. Briefly, after 24 hours of treatment with Fe3O4 (10mg/ml) cells were lysed with 70 µL of PhosphosafeTM; then, protein concentration (20 µg) was calculated by BCA protein analysis. Electrophoresis was performed using Nu-PAGE 10% SDSPAGE Bis-Tris gel in SDS-PAGE buffer. Polyvinylidene fluoride membrane (PVDF) was used for transfer. Next, membrane was blocked with bovine serum albumin (3%). Afterwards, membranes were washed with tris buffered saline containing tween 20 (TBST) and incubated overnight with primary antibody (procaspase-3, procaspase-9, Bcl-2, Bax and β-actin) diluted 1:1000. After that, membrane was washed three times with TBST and secondary antibody (1:1000) was added to be incubated for 1 hour

and washed with TBST. Then, band intensities were detected using chemiluminescent substrate Supersignal Femto kit and band densities were analyzed using ImageJ 1.52a program (Bethesda, Maryland, USA) [23].

Transmission Electron Microscopy (Tem) Analysis

The target HT-29 cells were collected and washed twice with PBS, and after fixing the cells with 2.5% glutaraldehyde and 2% paraformaldehyde at 4°C for 2 hours, the cells were coated with 1% osmium tetroxide. The cells were then dewatered with ethanol 30, 50, 70, 90, 100 and acetone 100, and then were placed in a resin for polymerization. Finally, sections of 70 nm were made and before selecting the appropriate section for TEM use, the cut samples (800 microns) were stained with Tluidin Blue and the appropriate area was selected with an optical microscope. Then, the samples were stained with 4% uranyl acetate and 2% lead citrate, and finally, images were taken with a transmission electron microscope in the central laboratory of Ferdowsi University of Mashhad, and 120 kV TEM image analysis was performed.

Flow Cytometry

The apoptosis and viability percentage test was performed by the Annexin V-FITC Apoptosis Staining / Detection Kit (ab14085). With this kit, there is no need to fix the cells and the living cell is stained directly. In fact, this method, on the one hand, identifies the cell population (here HT-29) in the early or final stages of apoptosis, and on the other hand, it differentiates the population of necrotic cells from living cells. Cells stained in this way can be detected by both flow cytometry and fluorescent microscopy. Preparation of HT-29 for flow cytometry was done according to the instructions of the corresponding company. Finally, the FLOW J V10 and graph pad version 8 software programs were used for analysis.

Nuclear Staining (DAPI)

DAPI (4 ' 6-Diamidino-2-phenylindole dihydrochloride) is a fluorescent dye that binds strongly to adenine-thymine-rich parts in DNA. With this dye, cells can be examined morphologically. To investigate the effect of L-phenyl alanine-coated magnetic iron oxide nanoparticles on HT-29 cell line after culturing cells in the presence of L-phenyl alanine-coated magnetic iron oxide nanoparticles after the required time, cells were gently washed with PBS and 1% formalin was added to fix the cells and refrigerated for 15 minutes at 4°C. The pellets were then exposed to the laboratory air at 27°C for 5 minutes. After formalin removal, 4% Triton was added to the samples to make the cell membrane permeable to DAPI dye. After 15 minutes and Triton extraction, the cells were washed with PBS and finally 1% DAPI dye of Denazist Asia Company was added to the cells. It should be noted that due to the sensitivity of DAPI dye to light, these steps were performed in the dark. Finally, cell morphology and changes due to the presence of NP Fe_3O_4 were examined by a blue fluorescence microscope. All steps were performed three times.

The inhibitory effect of Fe_3O_4 NP on HT-29 cell proliferation was examined by determining the degree of dermodoxyuridine participation in the DNA of HT-29 cells using Cell Proliferation ELISA kit, BrdU (colorimetric) and according to the manufacturer's protocol. The optical absorption of samples was read at the wavelength of 405 nm by the ELISA reader.

Number Of Cells

The number of HT-29 cells 24 hours after culturing with Fe_3O_4 was examined and the cells were photographed with an inverted microscope to record morphological changes and number of cells. The number of cells in the 24-hour group under the influence of L-phenyl alanine-coated magnetic iron oxide nanoparticles indicated a statistically significant decrease compared to the control group ($P < 0.05$). Also, morphologically, the shape of the cells was similar to apoptosis and degrade (Fig. 2B).

Intracellular And Extracellular Calcium Levels

Ca(2+) levels in HT-29 cells and cell culture medium were assessed. All reagents and solvents were provided from the German Merck company. Each sample was placed in a separate tube. Glass and plastic containers were soaked in 10% HNO3 for 24 hours and rinsed thoroughly with deionized water. All reagents used in the present study were highly purified and analytically suitable for trace element analysis. Standard solutions (1000 µg ml-1) of each element were employed using inductively coupled plasma optical emission spectrometry (ICP-OES) in the central laboratory of Ferdowsi University of Mashhad. Deionized water was used during the study to serially dilute the standards.

Results

NP Fe_3O_4 at concentrations above 2.5 causes cell date in HT-29 cells. First, HT29 cells were treated with Fe_3O_4 nanoparticles at concentrations of 5 to 2.5 µg / mL. Then, the percentage of cell viability after 48 hours was assessed. The results of cytotoxicity showed that treatment of HT29 cells with Fe_3O_4 at a rate of 2.5 µg / mL for 48 hours led to cell survival (Fig. 1b).

Fe_3O_4 reduces DNA replication and damage in HT-29 cells. In order to determine the effectiveness of Fe_3O_4 on proliferation and DNA structure, Brdu and Run tests on gel electrophoresis were used, respectively. Figure 1C shows that Fe_3O_4 reduces DNA replication and production in HT-29 cells by more than 49%. Figure 1D also shows that Fe_3O_4 destroys DNA in HT-29 cells.

Fe_3O_4 increases intracellular ROS and Ca in HT-29 cells. The results of ROS assay revealed that Fe_3O_4 increases the amount of ROS to 75% in treated cells (Fig. 1E). As illustrated in Fig. 1F, the amount of ca inside the treated cells is significantly higher than the control group cells ($p < 0.0001$).

Fe_3O_4 causes apoptosis in HT-29 cells. The results of flow cytometric analysis indicated that HT-29 cells had 15.9% apoptosis and 2.8% necrosis after 48 hours of treatment with Fe_3O_4 (Fig. 2A). The morphological image of the cell surface also showed that Fe_3O_4 enters the cell as a vesicle from the membrane surface, causing damage to the cell, which is also evident in the results of DAPI staining (Fig. 2C-E).

Fe_3O_4 increases Caspase 3 and 9 expression and decreases Bcl-2 expression in HT-29 cells. According to Figs. 3A1 and B1, the expression of Bax at the level of mRNA and protein in the group treated with Fe_3O_4 was not in statistical terms significantly different compared to the control group. However, caspase-9 showed a significant increase in mRNA and protein levels in the Fe_3O_4-treated group compared to the control group (Fig. 3A2 and B2). As seen in Figs. 3A3 and B3, the expression of caspase 3 at mRNA and protein levels was significantly higher in the treated group than in the control group ($P < 0.0001$). Nevertheless, the expression of Bcl-2 in Fe_3O_4-treated group significantly decreased at mRNA and protein levels in comparison with the control group ($P < 0.0001$) (Fig. 3, A4 and B4).

Discussion

This study demonstrated that Fe_3O_4 causes apoptosis in colon epithelial cells (HT-29). The results of MTT showed that Fe_3O_4 causes cell death in HT-29 in a dose-dependent manner. Fe_3O_4 also increases intracellular calcium, ROS, and DNA damage at concentrations studied to investigate apoptosis. A study by Kojima et al. (2018) showed that treatment of DU145 and PC-3 cancer cells with Fe_3O_4 increased ROS cell levels. The authors also concluded that treatment of both cell lines with 100 µg / ml Fe_3O_4 NP for 72 hours resulted in a significant inhibition of cell viability with different inhibitory effects [24]. Various studies have demonstrated that the mechanism of apoptosis by metal nanoparticles pertains to affecting ROS interactions in the treated cells [26 – 25]. Further, a study by Sato et al. (2013) showed that Fe_3O_4 can cause DNA damage [27].

Cellular uptake of Fe_3O_4 and cell structure studied in this research by a TEM electron microscope showed that Fe_3O_4 enters the cell through the cell surface vagules and causes apoptosis by various mechanisms. The results of various studies have revealed that the amount, manner, and place of Fe_3O_4 uptake can cause apoptosis [28–29].

The results of the present study indicated that the expression of caspase 3 and 9 in the Fe_3O_4 group increased compared to the control group and the expression of Bcl-2 decreased. A study by Chauhan et al. (2020) showed that Fe_3O_4 increases the expression of caspase-3 in lung cancer cells in a time-dependent manner [30].

Figure 4 shows the possible mechanisms of inducing apoptosis by Fe_3O_4 in the studied cells. It appears that Fe_3O_4 can cause apoptosis in three ways. The first and most important method is the direct destructive effect of DNA in HT-29 cells. Various studies have demonstrated that DNA damage increases

the expression of factors such as P53 and subsequently leads the cell to apoptosis [31–32]. Moreover, Fe_3O_4 increases ROS levels, which in turn causes apoptosis in several ways. Most nano-drugs have been shown to increase cytochrome C by increasing ROS and affecting mitochondria. The increased cytochrome C augments the activation of caspases 3 and 7, which leads to apoptosis [33–35]. ROS also releases lysosomes that can play a role in apoptosis [36–37]. In addition, in this study, it was found that Fe_3O_4 increases intracellular calcium by causing oxidative stress, which following the increase in intracellular calcium levels can open mitochondrial pores in a mechanism similar to ROS, causing cytochrome C to exit and inducing apoptosis [38–39]. Other important results of the present study were the increase in caspase 3 and 9 expression and the decrease in Bcl-2 expression. It seems that Fe_3O_4 increases the expression of caspases 3 and 9 and decreases the expression of Bcl-2 through DNA damage and indirect effect on mitochondria. [40–42].

Conclusion

Fe_3O_4 causes apoptosis in cancer cells by increasing the level of ROS and intracellular calcium, followed by increasing the expression of caspases 3 and 9 and decreasing the expression of Bcl-2, as well as direct DNA damage. All these indicate that Fe_3O_4 can be a suitable chemotherapy drug with a wide range of side effects, and in order to eliminate the side effects, its specific mode of transmission is very important.

Declarations

This article does not contain any studies with human participants. All animals used in this study were purchased from market, and the experimental protocols adhered to the guidelines of the Declaration of Helsinki.

Compliance with ethical standards

Conflict of interest all authors declare that they have no conflict of interest.

Data availability

Data and material are available upon reasonable request.

References

1. Ranjbary AG, Mehrzad J, Dehghani H, Abdollahi A, Hosseinkhani S. (2020). Variation in Blood and Colorectal Epithelia's Key Trace Elements along with Expression of Mismatch Repair Proteins from Localized and Metastatic Colorectal Cancer Patients. Biol Trace Elem Res. 194(2):629.

2. Mauri G, Sartore-Bianchi A, Russo AG, Marsoni S, Bardelli A, Siena S. (2019). Early-onset colorectal cancer in young individuals. Mol Oncol. 13(2):109-131.

3. Siegel RL, Jakubowski CD, Fedewa SA, Davis A, Azad NS. (2020). Colorectal Cancer in the Young: Epidemiology, Prevention, Management. Am Soc Clin Oncol Educ Book. 40:1-14.

4. Arruebo M, Vilaboa N, Sáez-Gutierrez B, Lambea J, Tres A, Valladares M, González-Fernández A. (2011). Assessment of the evolution of cancer treatment therapies. Cancers (Basel). 3(3):3279-330.

5. Hassanzadeh P, Fullwood I, Sothi S, Aldulaimi D. (2011). Cancer nanotechnology. Gastroenterol Hepatol Bed Bench. 4(2):63-9.

6. Boateng F, Ngwa W. (2019). Delivery of Nanoparticle-Based Radiosensitizers for Radiotherapy Applications. Int J Mol Sci. 21(1):273.

7. Zhao CY, Cheng R, Yang Z, Tian ZM. (2018). Nanotechnology for Cancer Therapy Based on Chemotherapy. Molecules. 23(4):826.

8. Ali A, Zafar H, Zia M, Ul Haq I, Phull AR, Ali JS, Hussain A. (2016). Synthesis, characterization, applications, and challenges of iron oxide nanoparticles. Nanotechnol Sci Appl. 9:49-67.

9. Ganapathe LS, Mohamed MA, Mohamad Yunus R, Berhanuddin DD. (2020). Magnetite (Fe3O4) Nanoparticles in Biomedical Application: From Synthesis to Surface Functionalisation. Magnetochemistry. 6(4):68.

10. Namvar F, Rahman HS, Mohamad R, Baharara J, Mahdavi M, Amini E, Chartrand MS, Yeap SK. (2014). Cytotoxic effect of magnetic iron oxide nanoparticles synthesized via seaweed aqueous extract. Int J Nanomedicine. 9:2479-88.

11. Kanagesan S, Hashim M, Tamilselvan S, Alitheen NB, Ismail I, Hajalilou A, Ahsanul K. (2013). Synthesis, characterization, and cytotoxicity of iron oxide nanoparticles. Advances in Materials Science and Engineering. 2013.

12. Wu M, Huang S. (2017). Magnetic nanoparticles in cancer diagnosis, drug delivery and treatment. Mol Clin Oncol. 7(5):738-746.

13. Manke A, Wang L, Rojanasakul Y. (2013). Mechanisms of nanoparticle-induced oxidative stress and toxicity. BioMed research international. 2013.

14. Yu Z, Li Q, Wang J, Yu Y, Wang Y, Zhou Q, Li P. (2020). Reactive Oxygen Species-Related Nanoparticle Toxicity in the Biomedical Field. Nanoscale Res Lett. 15(1):115.

15. Erofeev A, Gorelkin P, Garanina A, Alova A, Efremova M, Vorobyeva N, Edwards C, Korchev Y, Majouga A. (2018). Novel method for rapid toxicity screening of magnetic nanoparticles. Scientific reports. 8(1):1-1.

16. Huang YW, Cambre M, Lee HJ. (2017). The Toxicity of Nanoparticles Depends on Multiple Molecular and Physicochemical Mechanisms. Int J Mol Sci. 18(12):2702.

17. Lujan H, Sayes CM. (2017). Cytotoxicological pathways induced after nanoparticle exposure: studies of oxidative stress at the 'nano-bio' interface. Toxicol Res (Camb). 6(5):580-594.

18. Fu PP, Xia Q, Hwang HM, Ray PC, Yu H. (2014). Mechanisms of nanotoxicity: generation of reactive oxygen species. Journal of food and drug analysis. 22(1):64-75.

19. Yu Z, Li Q, Wang J, Yu Y, Wang Y, Zhou Q, Li P. (2020). Reactive oxygen species-related nanoparticle toxicity in the biomedical field. Nanoscale research letters. 15:1-4.

20. Rashid H, Mansoor MA, Haider B, Nasir R, Abd Hamid SB, Abdulrahman A. (2020). Synthesis and characterization of magnetite nano particles with high selectivity using in-situ precipitation method. Separation Science and Technology. 55(6):1207-15.

21. Lodhia J, Mandarano G, Ferris NJ, Eu P, Cowell SF. (2010). Development and use of iron oxide nanoparticles (Part 1): Synthesis of iron oxide nanoparticles for MRI. Biomedical imaging and intervention journal. 6(2):e12.

22. Hebling J, Bianchi L, Basso FG, Scheffel DL, Soares DG, Carrilho MR, Pashley DH, Tjäderhane L, de Souza Costa CA. (2015). Cytotoxicity of dimethyl sulfoxide (DMSO) in direct contact with odontoblast-like cells. Dent Mater. 31(4):399-405.

23. Zhang L, Chen H, Wang M, Song X, Ding F, Zhu J, Li X. (2018). Effects of glabridin combined with 5-fluorouracil on the proliferation and apoptosis of gastric cancer cells. Oncology letters. 15(5):7037-45.

24. Kojima K, Takahashi S, Saito S, Endo Y, Nittami T, Nozaki T, Sobti RC, Watanabe M. (2018). Combined effects of Fe3O4 nanoparticles and chemotherapeutic agents on prostate cancer cells in vitro. Applied Sciences. 8(1):134.

25. Manke A, Wang L, Rojanasakul Y. (2013). Mechanisms of nanoparticle-induced oxidative stress and toxicity. Biomed Res Int. 942916.

26. Jawaid P, Rehman MU, Zhao QL, Misawa M, Ishikawa K, Hori M, Shimizu T, Saitoh JI, Noguchi K, Kondo T. (2020). Small size gold nanoparticles enhance apoptosis-induced by cold atmospheric plasma via depletion of intracellular GSH and modification of oxidative stress. Cell death discovery. 6(1):1-2.

27. Sato A, Itcho N, Ishiguro H, Okamoto D, Kobayashi N, Kawai K, Kasai H, Kurioka D, Uemura H, Kubota Y, Watanabe M. (2013). Magnetic nanoparticles of Fe3O4 enhance docetaxel-induced prostate cancer cell death. Int. J. Nanomedicine. 8:3151.

28. Shen S, Liu Y, Huang P, Wang J. (2009). In vitro cellular uptake and effects of Fe3O4 magnetic nanoparticles on HeLa cells. J Nanosci Nanotechnol. 9(5):2866-71.

29. Mustafa T, Watanabe F, Monroe W, Mahmood M, Xu Y, Saeed LM, Karmakar A, Casciano D, All S, Biris AS. (2011). Impact of gold nanoparticle concentration on their cellular uptake by MC3T3-E1 mouse osteoblastic cells as analyzed by transmission electron microscopy. J. Nanomed. Nanotechnol. 2(6):1000118.

30. Chauhan A, Kumar R, Singh P, Jha SK, Kuanr BK. (2020). RF hyperthermia by encapsulated Fe3O4 nanoparticles induces cancer cell death via time-dependent caspase-3 activation. Nanomedicine. 15(04):355-79.

31. Ozaki T, Nakagawara A. (2011). Role of p53 in Cell Death and Human Cancers. Cancers (Basel). 3(1):994-1013.

32. Elmore S. (2007). Apoptosis: a review of programmed cell death. Toxicol Pathol. 35(4):495-516.

33. Ivanova D, Zhelev Z, Aoki I, Bakalova R, Higashi T. (2016). Overproduction of reactive oxygen species - obligatory or not for induction of apoptosis by anticancer drugs. Chin J Cancer Res. 28(4):383-96.

34. Ott M, Gogvadze V, Orrenius S, Zhivotovsky B. (2007). Mitochondria, oxidative stress and cell death. Apoptosis. 12(5):913-22.

35. Kasai S, Shimizu S, Tatara Y, Mimura J, Itoh K. (2020). Regulation of Nrf2 by mitochondrial reactive oxygen species in physiology and pathology. Biomolecules. 10(2):320.

36. Dielschneider RF, Henson ES, Gibson SB. (2017). Lysosomes as Oxidative Targets for Cancer Therapy. Oxid Med Cell Longev. 3749157.

37. Redza-Dutordoir M, Averill-Bates DA. (2016). Activation of apoptosis signalling pathways by reactive oxygen species. Biochimica et Biophysica Acta (BBA)-Molecular Cell Research. 1863(12):2977-92.

38. Giorgi C, Baldassari F, Bononi A, Bonora M, De Marchi E, Marchi S, Missiroli S, Patergnani S, Rimessi A, Suski JM, Wieckowski MR, Pinton P. (2012). Mitochondrial Ca(2+) and apoptosis. Cell Calcium. 52(1):36-43.

39. Feno S, Butera G, Vecellio Reane D, Rizzuto R, Raffaello A. (2019). Crosstalk between calcium and ROS in pathophysiological conditions. Oxid. Med. Cell. Longev. 24;2019.

40. Zhu L, Han MB, Gao Y, Wang H, Dai L, Wen Y, Na LX. (2015). Curcumin triggers apoptosis via upregulation of Bax/Bcl-2 ratio and caspase activation in SW872 human adipocytes. Mol Med Rep. 12(1):1151-6.

41. Alarifi S, Ali H, Saad Alkahtani MS. (2017). Regulation of apoptosis through bcl-2/bax proteins expression and DNA damage by nano-sized gadolinium oxide. Int. J. Nanomedicine. 12:4541.

42. Yue J, López JM. (2020). Understanding MAPK signaling pathways in apoptosis. Int. J. Mol. Sci. 21(7):2346.

Figures

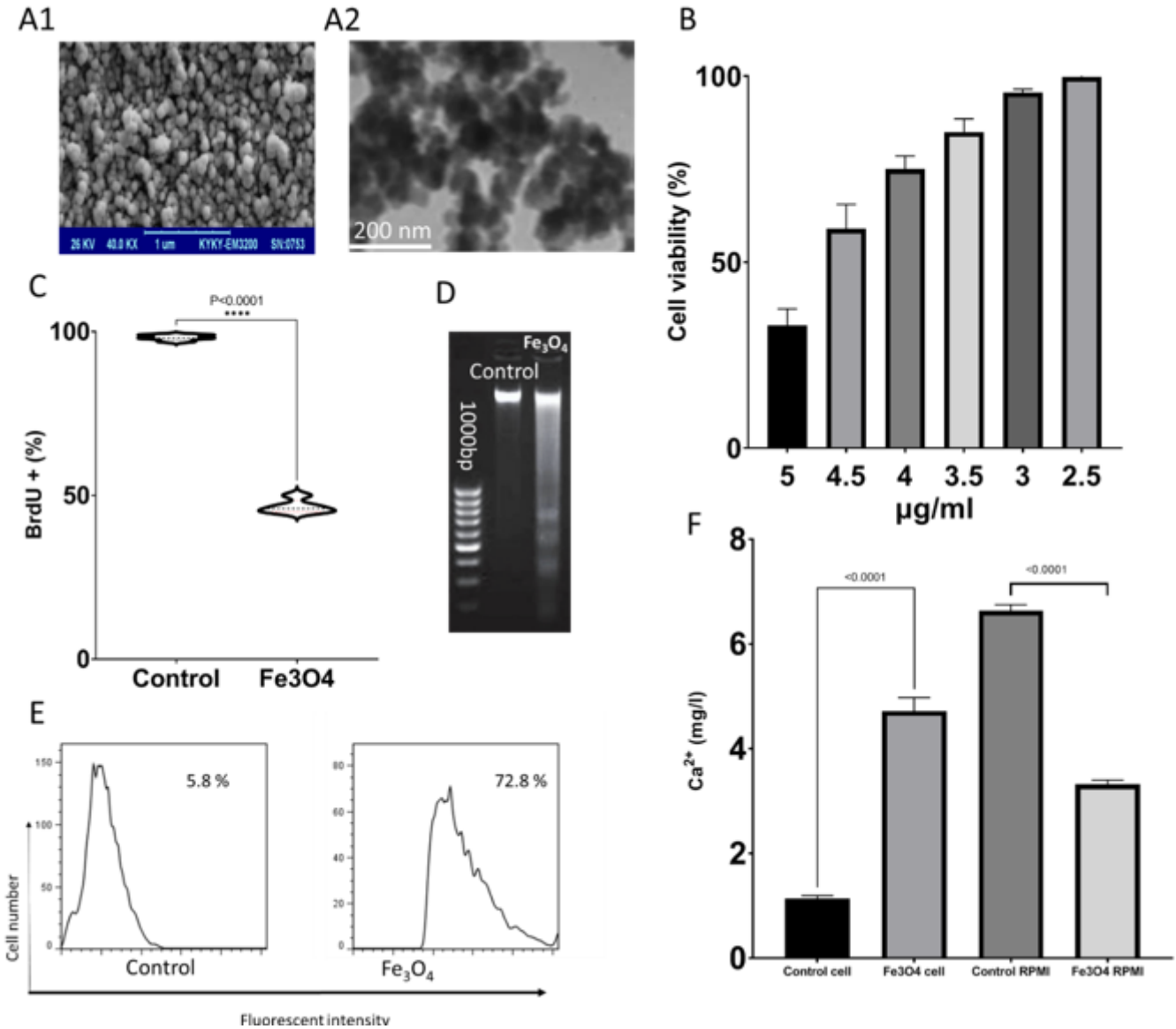

Figure 1

A, Transmission electron microscopy of Fe3O4 nanoparticles. Magnification, x100,000; B HT-29 cell viability after exposing to Fe3O4 nanoparticles; C Effect of Fe3O4 on 5-bromo-2'-deoxyuridine (BrdU) incorporation in HT-29 cells, each bar represents the mean ± SEM (n = 5). *** Different from 0 µg/mL, P < 0.0001. D, Analysis of intranucleosomal DNA fragmentation of HT29 cells with Fe3O4 nanoparticles; E, Flow cytometry with dichlorodihydrofluorescein diacetate (DCFDA) dye to measure the amount of

reactive oxygen species (ROS) in HT-29 cells; F, The amount of ca in the HT-29 cells treated with Fe3O4 nanoparticles.

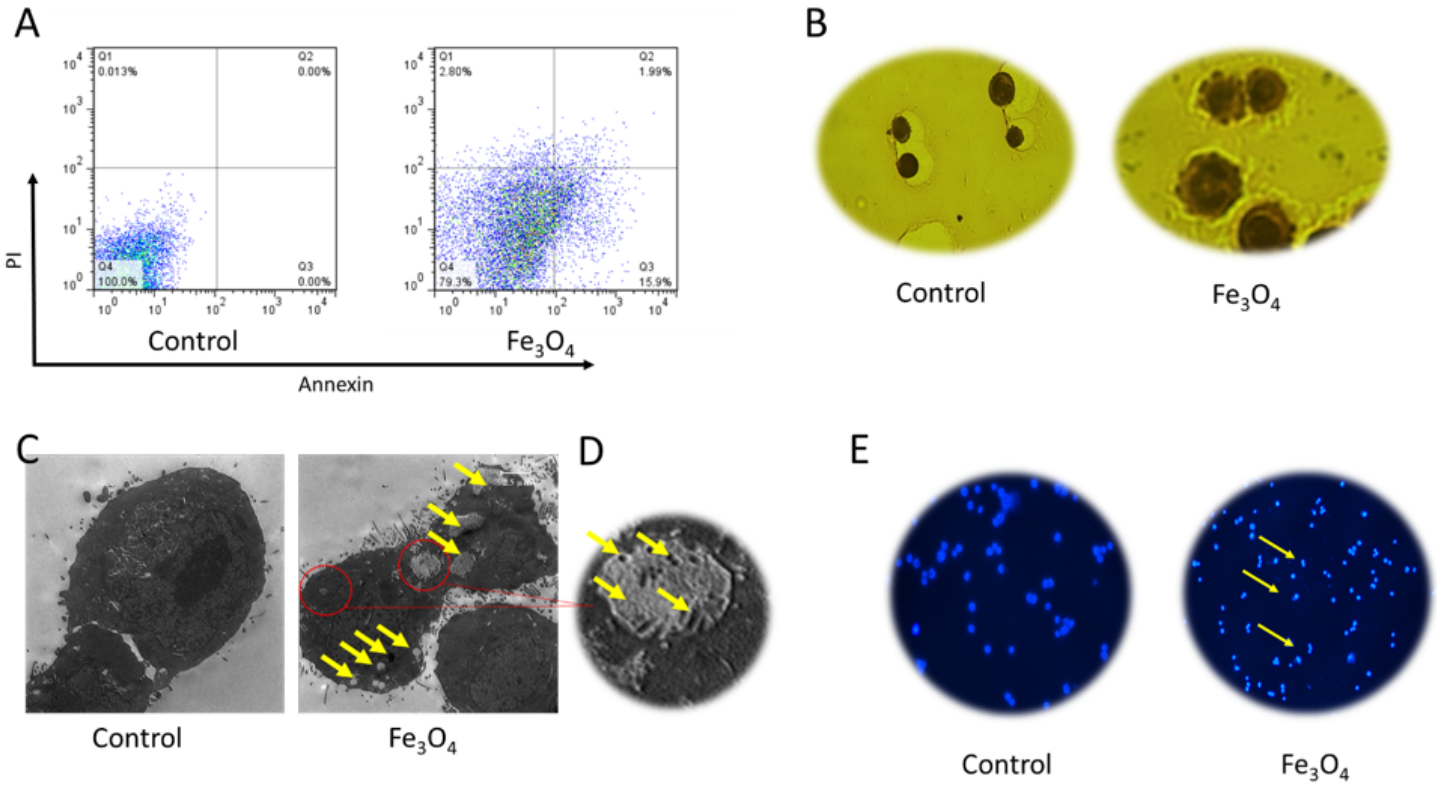

Figure 2

A, Apoptosis assay using flow cytometry after staining with annexin V-FITC/propidium iodide (PI); B, microscopic figure (100x magnification); C, HT-29 cells were observed by TEM (×5000) and the arrows indicate the apoptotic bodies; E, DAPI staining of HT-29 cells and arrow represents the DNA changes caused by apoptosis in the examined cells.

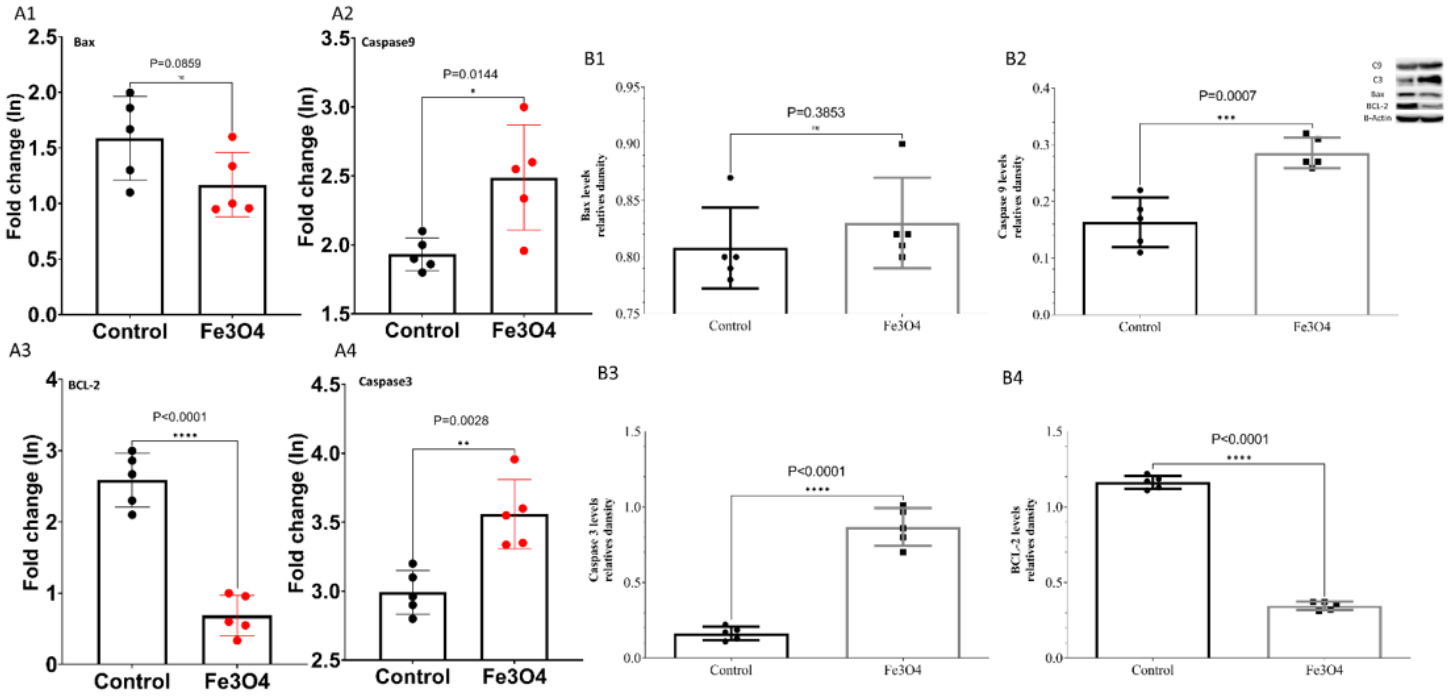

Figure 3

Fe3O4 nanoparticles -induced apoptosis includes an increase in caspase 3 and 9 and a decrease in Bcl-2 expressions. A, mRNA, Bax, Bcl-2, C3 and C9 results obtained by RT-PCR; B, Bax, Bcl-2, C3 and C9 expression results obtained by western blot in HT-29 cells.

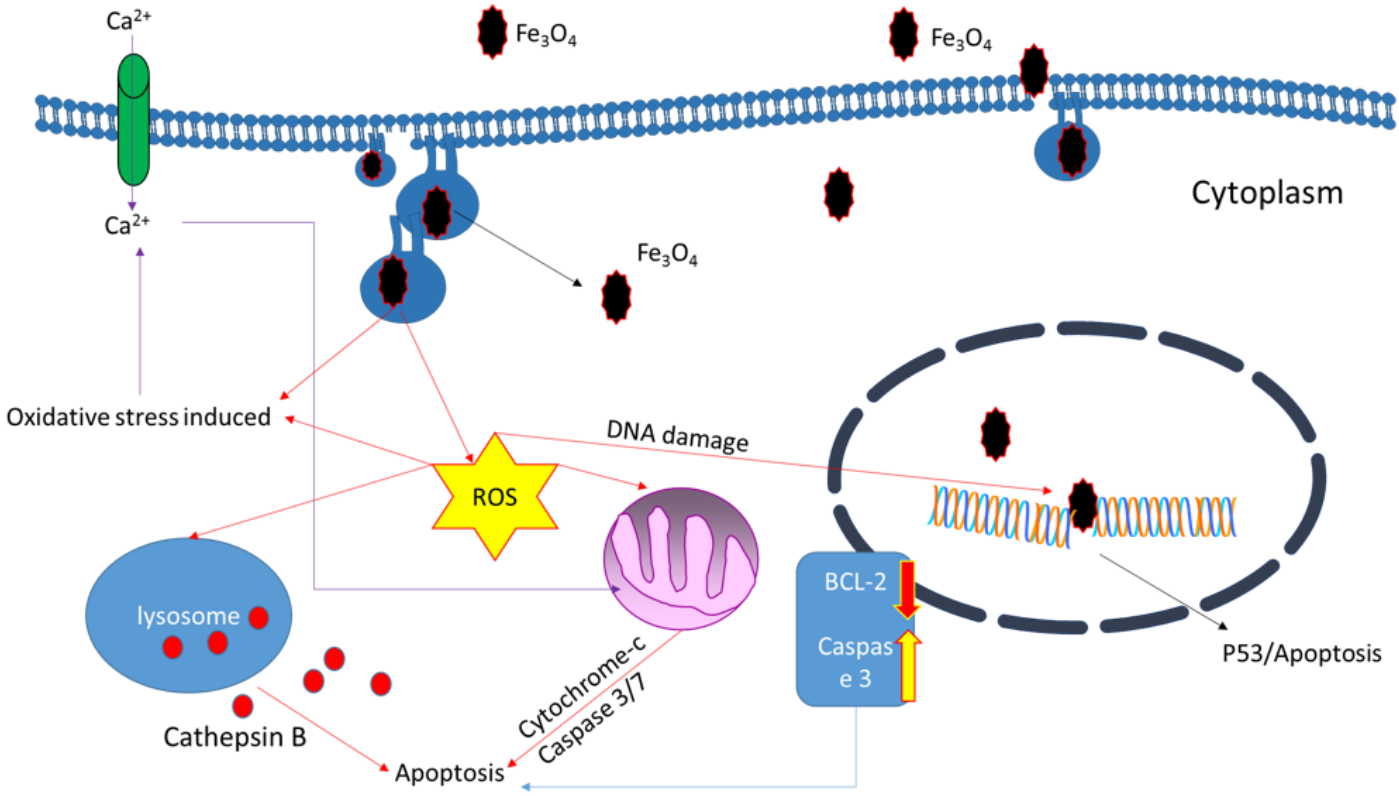

Figure 4

A hypothesis for toxic mechanism following uptake of Fe3O4 nanoparticles.